Available online at www.sciencedirect.com
SCIENCE DIRECT®
Journal of Solid State Chemistry 179 (2006) 476–485
JOURNAL OF SOLID STATE CHEMISTRY
www.elsevier.com/locate/jssc

The chemical changes occurring upon cycling of a SnO_2 negative electrode for lithium ion cell: In situ Mössbauer investigation

I. Sandu[a], T. Brousse[a,**], D.M. Schleich[a], M. Danot[b,*]

[a]*Laboratoire de Génie des Matériaux et Procédés Associés (EA 2664), école polytechnique de l'Université de Nantes, La Chantrerie, rue Christian Pauc, BP 50609, 44306 Nantes Cedex 3, France*

[b]*Laboratoire de Chimie des Solides, Institut des Matériaux Jean Rouxel, UMR 6502, CNRS-Université de Nantes, 2 rue de la Houssinière, BP 32229, 44322 Nantes Cedex 3, France*

Received 29 March 2005; received in revised form 26 October 2005; accepted 26 October 2005
Available online 15 December 2005

Abstract

Electrochemical reduction of a SnO_2 electrode for a lithium ion cell is known to result in formation of $Li_{4.4}Sn$ alloy + $2Li_2O$. In order to determine to which extent such an electrode can be considered as reversible, we studied the electrochemical oxidation of a previously reduced SnO_2 electrode, using in situ ^{119}Sn Mössbauer spectroscopy. Contrary to what could be expected, the first step does not consist in extraction of lithium from $Li_{4.4}Sn$ for β-Sn to be obtained. In fact, simple lithium extraction proceeds only down to the $Li_{1.4}Sn$ composition. Further oxidation (second step) involves formation of unusual species (Sn(0) and oxygen-surrounded Sn(II), both probably in interaction with Li_2O). Then (third step), red SnO-like Sn(II) species are formed, along with some Sn(IV). Especially during the second and third steps, the working electrode is far from thermodynamic equilibrium despite the low oxidation rate. This non-equilibrium behavior is probably related to the ultrafine particle size resulting from electrochemical grinding.

Keywords: In situ; Mössbauer spectroscopy; ^{119}Sn; Tin dioxide; Negative electrode; Lithium ion

1. Introduction

In a previously published paper [1] we reported on the chemical changes that occur during the first reduction of a SnO_2 electrode for a lithium ion cell (cell discharge). This work, based on an in situ ^{119}Sn Mössbauer study, allowed the chemical mechanism proposed by Courtney [2] ($SnO_2 \rightarrow \beta$-$Sn \rightarrow Li_ySn$) to be precised. We showed that the first reaction step consists in lithium intercalation into the SnO_2 host lattice, which had never been reported to occur in an operating SnO_2 electrode, and that the reduction mechanism cannot be described as a succession of well-defined stages since we observed important imbrication of the different steps (lithium intercalation, reduction of more or less lithiated SnO_2 into unusual Sn(II) and/or Sn(0) species, Li_ySn alloy formation). Besides, comparison of these results [1] with those of the Mössbauer ex situ study we previously performed at low temperature (78 K) on the same system [3] shows that unusual species observed in situ were not evidenced in the ex situ spectra. It suggests that these unusual species either rapidly transformed into usual stable ones or were accidentally oxidized during the transfer of the electrode from the battery to the Mössbauer sample holder (the atmosphere of a glove box can never be considered as perfectly inert). This point, among others, clearly evidences the usefulness of in situ measurements for the study of such dynamic systems (Ref. [1] gives more details concerning the interest of in situ Mössbauer measurements in such cases). We consequently thought it would be interesting to study in the same way the phenomena occurring during the SnO_2 electrode reoxidation (charge of lithium ion cell) in order to determine to which extent such an electrode can be considered as reversible. In particular, Courtney [2] first proposed reoxidation to stop when the Li_ySn alloys are

**Also for correspondence. Fax: +33 2 40 68 31 99
*Corresponding author. Fax: +33 2 40 37 39 95.
E-mail addresses: thierry.brousse@polytech.univ-nantes.fr (T. Brousse), michel.danot@cnrs-imn.fr (M. Danot).

0022-4596/$ - see front matter © 2005 Elsevier Inc. All rights reserved.
doi:10.1016/j.jssc.2005.10.042

completely transformed into β-Sn, but then, studying SnO-based electrodes, he evidenced at the end of the reduction–oxidation cycle the presence of β-Sn, Sn(II), and Sn(IV) [4]. In our ex situ study [3], we observed these same species in the reoxidized electrode. However, we cannot be sure that Sn(II) and Sn(IV) were effectively formed upon the electrode oxidation since, due to the sensitivity of small metallic particles to oxygen or water traces, their presence could result from partial accidental oxidation of β-Sn during the transfer of our material into the Mössbauer sample holder. Besides, referring to the SnO_2 electrode reduction study [1,3], it can be thought that unusual species also can be involved in the subsequent oxidation, even if their presence was not evidenced by the ex situ Mössbauer results [3]. Only in situ measurements are able to allow these particular points and, more generally, the electrode reoxidation mechanism to be clarified.

2. Experimental

The battery we used for our in situ Mössbauer study was prepared according to the plastic technology [5] by the Laboratoire de Réactivité et de Chimie des Solides, Unité de Prototypage UMR 6007 CNRS, Amiens. In fact, this battery is the one that led to the results concerning the SnO_2 electrode reduction we reported in a previous paper [1]. After its reduction, the electrode was submitted to reoxidation (lithium extraction), which is the subject of the present article.

The electrode oxidation (3 weeks) was monitored by a MacPile device operating according to the potentiostatic mode. The potential was varied step by step (10 mV/3 h) and the current continuously measured in order to allow, through integration, the amount of extracted lithium to be determined, and x, the lithium amount (per Sn mole) remaining in the electrode, to be deduced.

The ^{119}Sn Mössbauer measurements were performed using a conventional constant acceleration spectrometer equipped with a $Ca^{119m}SnO_3$ source (5 mCi). The velocity scale was calibrated with two reference absorbers, β-Sn and $CaSnO_3$. The isomer shifts are referred to $CaSnO_3$ at room temperature. The typical acquisition time was about 24 h per spectrum. The amount of remaining lithium (x Li per Sn mole) corresponding to each of the spectra (and used in the text and the figures) is calculated as the average value between the lithium contents at the beginning and at the end of the acquisition time.

Least-squares refinement of the parameters was performed using lorentzian line shape. Both individual lines of any quadrupole doublet were constrained to have equal linewidth and absorption depth. Most of our spectra contain several unresolved contributions. In these conditions, attempts to refine all the parameters can give meaningless results. First of all, for the spectra consisting of two quadrupole doublets with largely different intensities, refinement of the linewidth of the minor contribution can give abnormal values. In this case, it was necessary to fix this linewidth at a reasonable value, a value refined for a spectrum where this component is more intense if possible. For spectra consisting of more than two contributions, even refinement of some position parameters (isomer shift and quadrupole splitting) can be hazardous. In this case, it was necessary too to fix the concerned parameters at a reasonable value derived from the refinement of another spectrum for which it is meaningful. In such a situation, it was of course logical to fix the corresponding linewidth(s) also. The problem of refining position parameters is discussed in the sections where it arises. As for the linewidths, when refined (and when fixed at a value derived from another spectrum), they range from 0.90 to 1.10 mm/s (2Γ = FWHM). In the few cases for which reference to another spectrum is impossible, 2Γ was fixed to 1.00 mm/s.

All the in situ spectra were of course recorded at room temperature. It has to be kept in mind that, for such a rather high measuring temperature, some difficulties can be encountered concerning identification of phases with a low recoilless fraction (f, Lamb–Mössbauer factor) and determination of the relative amounts of phases with different f values.[1]

3. Results and discussion

As previously reported [1], the reduction of our SnO_2 electrode required the reaction of 8.4 Li per mole of Sn and finally resulted in the formation of Li_ySn alloy. The reduction reaction can thus be globally represented as follows:

$$SnO_2 + 8.4\ Li \rightarrow 2\ Li_2O + Li_{4.4}Sn.$$

Consequently, when the subsequent oxidation begins (present article), the electrode contains lithium oxide (2 mol per Sn mole) and the $Li_{4.4}Sn$ alloy (i.e. $Li_{22}Sn_5$, in agreement with Weng's results [6]). Alternatively, based on more recent work by Goward et al. [7], a value of 4.25 Li per mol of Sn can be found in the literature for the lithium-richest alloy ($Li_{17}Sn_4$) in the reduced SnO_2 electrode. To be consistent with our measurements, we will hereafter use the formulation $Li_{4.4}Sn$.

[1]Only the f fraction of the ^{119}Sn nuclei contributes to the Mössbauer spectrum since Mössbauer effect is based on recoilless resonant absorption of γ-rays by nuclei. The $(1-f)$ remaining fraction dissipates the total recoil energy of the system as lattice vibrations and thus cannot contribute to the resonant absorption. The recoilless fraction reflects the dynamics of the tin-containing lattice. At a given measurement temperature, it is higher if the lattice is more rigid, i.e. if Sn is involved in strong bonds. For a given compound, decrease of the measurement temperature attenuates the lattice vibrations and thus increases f. If tin is present in proportions $p(i)$ in several (i) species in a sample which contains a total of N tin atoms, the contribution of each of these species, Abs(i), to the total absorption area (AbsTot = ΣAbs(i)) is proportional to $p(i) \times N \times f(i)$. For this reason, the $p(i)$ proportions of tin in the different species can be deduced from the corresponding Abs(i) areas only if the $f(i)$ values are known.

3.1. Does the electrode oxidation simply involve transformation of $Li_{4.4}Sn$ into Sn(0)?

(We prefer to write "Sn(0)" rather than "β-Sn" or "metallic Sn" because appellation "Sn(0)" is more general and can include unusual species).

Most of our Mössbauer spectra contain several unresolved components. For this reason, their interpretation is not always straightforward, as already noted in our previous study [1]. In such cases, the variation of the total absorption area can provide valuable help, as far as the chemical changes that occur induce variation of the Lamb-Mössbauer factor (f) of the Mössbauer nuclei (for instance, transformation of species with low f value into species with high f value results in the increase of the absorption area). Effectively, during the SnO_2 electrode reduction [1], it is the absorption area variation that allowed lithium intercalation to be evidenced as the first reaction step. Besides, for higher lithium amounts, a close relation was observed between the absorption areas and the melting points (lattice rigidity) of the various Li_ySn alloys. An interesting aspect of the total absorption area values is that their determination only requires the experimental spectra to be reproduced as perfectly as possible, even if the chosen models do not represent chemical reality. We calculated in this way the absorption areas for all the spectra we recorded during the electrode oxidation and normalized the different values to the background count numbers of the corresponding spectra, in order to obtain "NormAbs" values independant of the acquisition time (which is not the same for the various spectra). Fig. 1 represents the NormAbs variation versus x, the amount of lithium per Sn mole remaining in the electrode. Since oxidation consists in lithium extraction, it proceeds from the right to the left of the x scale; it begins at $x = 8.4$, the lithium content at the end of reduction.

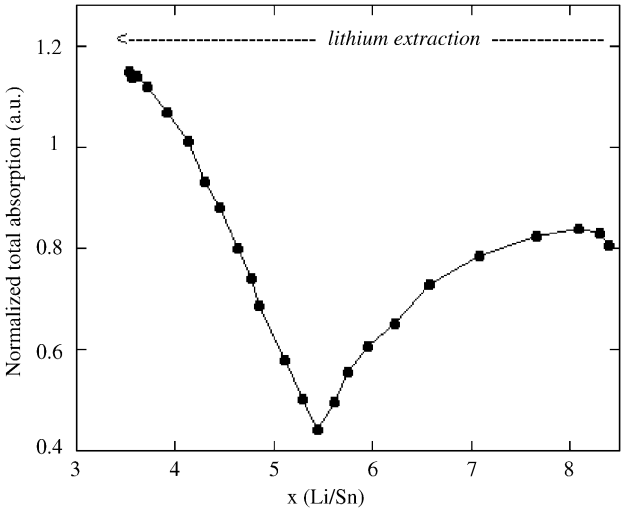

Fig. 1. Variation of the normalized total absorption area during oxidation of the previously reduced SnO_2 electrode. The lines are guide for the eyes. The error bar is 0.04.

First of all, it unambiguously appears that chemical changes concern lithium contents ranging from 8.4 to $\approx$3.6 Li per Sn mole, which means that the amount of extracted lithium is $\approx$4.8 Li per Sn mole. It follows that the result of the oxidation cannot be pure metallic tin, whose formation from $Li_{4.4}Sn$ would require extraction of only 4.4 Li/Sn.

More oxidized species (Sn(II) and/or Sn(IV)) are thus necessarily present in the electrode at the end of the oxidation. It means that the lithium oxide formed upon reduction of the SnO_2 electrode partly dissociates upon oxidation of the tin-containing material, which results in the formation of Sn(II)–O and/or Sn(IV)–O contacts and removal of more than 4.4 Li per Sn mole. Such a behavior has already been observed for transition metal oxide electrodes upon reoxidation [8] and was previously suspected from our early work on SnO_2, using ex situ analytical techniques [3].

From $x = 8.4$ to $x \approx 5.4$, NormAbs first slightly increases and then more and more drastically decreases. Analogous composition dependence of NormAbs was already observed during the formation of the Li_ySn alloys (reduction of the SnO_2 electrode) [1]. As discussed in Ref. [1], this variation can be explained by a similar variation of the f factor. Effectively, when y decreases from 4.4 to 0, the melting point of well-defined Li_ySn alloys first slightly increases and then more and more drastically decreases; the room temperature f factor (and consequently NormAbs), which depends upon the lattice rigidity, logically varies with the lithium content in the same way as the melting point does [1,4,9,10]. In this region ($8.4 > x > 5.4$), the NormAbs variation thus indicates that lithium is progressively extracted from the alloys.

For x decreasing from $\approx$5.4, NormAbs drastically increases, which means that the oxidation mechanism now involves the formation of species with higher f values. It follows that the first step of the oxidation cannot consist in the transformation $Li_{4.4}Sn \rightarrow \beta$-Sn (followed, in a second step, by oxidation of Sn to Sn(II) and/or Sn(IV)). Effectively, if it was the case and keeping in mind the very low f value of metallic tin, NormAbs should decrease not down to $x = 5.4$ but down to $x = 4$ (extraction of 4.4 Li/Sn) and then increase due to formation of Sn(II) or Sn(IV), whose f factors are much greater than that of metallic Sn. This plot thus clearly demonstrates that simple extraction of lithium from the alloys proceeds on a 3 Li range (8.4–5.4) and that a new phenomenon occurs when the alloy reaches the composition $Li_{1.4}Sn$ ($x = 5.4$). The NormAbs increase observed for $x < 5.4$ thus suggests that Sn(II) and/or Sn(IV) begin to form before lithium is totally removed from the Li_ySn alloys. Assuming only Sn(II) to be formed, the alloy oxidation should be globally represented as follows:

$$Li_{4.4}Sn + 2\ Li_2O \rightarrow SnO + Li_2O + 6.4\ Li,$$

and should proceed down to $x = 2$ (6.4 Li extracted). Now, our experiments show the oxidation to be finished before, at $x = 3.6$. It means that formation of tin oxides (SnO and, with greater reason, SnO_2) cannot be total. Sn(0) and/or lithium-poor alloys are thus necessarily present at the end of the oxidation, but the absorption decrease they can be expected to induce is largely over-compensated by the absorption increase related to the formation of the high f Sn(II) and/or Sn(IV) species.

All the assumptions listed above must be examined in the light of previous works on SnO_2 electrodes [11–18]. First of all, most of the papers issued in this field show that, as observed in our study, the first discharge of the SnO_2 electrode leads to the formation of $Li_{22}Sn_5$. Besides, according to these previous works, it seems that, upon reoxidation, some parts of the Li-rich Li_ySn alloys become electrochemically inactive because they soon disconnect from the electronic conducting pathway due to the electrochemical grinding related to the important volumic contraction (in β-Sn, the volume per Sn atom is less than one-third (28%) of that in $Li_{22}Sn_5$). As a result, residual Li-rich alloys can be present in the electrode, even when the X-ray diffraction pattern only consists of the β-Sn lines. These (broadened) lines indicate that β-Sn is surely present, but this does not mean that it is the unique tin-containing constituent of the electrode at this stage of charge since poorly crystallized or amorphous compounds cannot be detected by this technique.

In the present study, it is clear that no significant amount of Li-rich Li_ySn alloy was let apart upon reoxidation of the electrode, since the f factor of such compounds is strong enough for an eventual residual component to be observed in the Mössbauer spectra, which is not the case. The reason for this "unusual" behavior is probably that the cycling rate we used is much slower than in most of the reported studies.

Considering the previous remarks and without looking at any spectrum, one can deduce from Fig. 1 that the electrode oxidation proceeds in two steps:

- firstly, $Li_{4.4}Sn$ transforms into $Li_{1.4}Sn$;
- secondly, $Li_{1.4}Sn$ transforms into Sn(II) and/or Sn(IV) along with lithium-poorer alloy(s) and/or Sn(0).

The transition between the two corresponding domains is probably responsible for the slope change in the vicinity of $x = 5.5$ on the potentiostatic curve recorded during the electrode oxidation (Fig. 2a).

Even if the NormAbs variation provides valuable information, it cannot allow the nature of the reaction products involved during the electrode oxidation to be established. The usual deconvolution procedure will allow the oxidation process to be precised hereafter through discussion of the parameters refined for the different spectra.

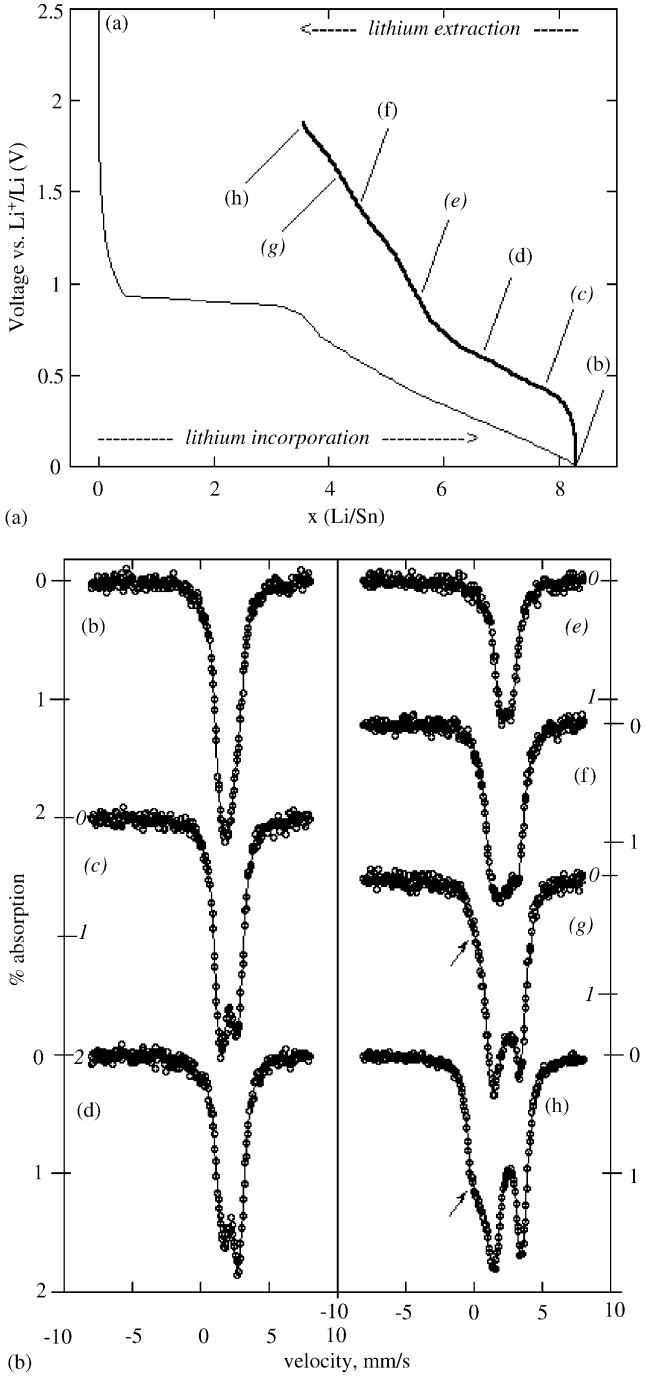

Fig. 2. (a) Potentiostatic curve recorded during reduction (plain line) of the SnO_2 electrode [1] and subsequent oxidation (bold line, present work). Letters (b)–(h) refer to the corresponding Mössbauer spectra. (b)–(h) ^{119}Sn Mössbauer spectra recorded during oxidation of the previously reduced SnO_2 electrode : $x = 8.40$ (b), 7.66 (*c*), 6.58 (d), 5.45 (*e*), 4.63 (f), 4.13 (*g*), 3.56 (h). For clarity purpose, plain and italic types are alternately used for (b)–(h), and for the corresponding absorption scales. The contribution of Sn(IV) to spectra (g) and (h) is indicated by the arrows.

3.2. Simple extraction of lithium from the Li_ySn alloys ($8.4 > x > 5.4$, i.e. $4.4 > y > 1.4$)

The spectra recorded in the region ranging from $x = 8.4$ to $x \approx 5.9$ are asymmetric singlets (Fig. 2b) or broadened

asymmetric doublets (Figs. 2c and d), which shows in both cases that several tin sites are present. Since they are unresolved, we thought it would be meaningless to consider an excessive number of variables [1] and introduced in our calculations the minimum site number for good reproduction of the experimental data to be achieved (as we already did in our study of the SnO_2 electrode reduction [1]). Two quadrupole doublets are enough for all these spectra to be correctly simulated. For x ranging from ≈ 5.9 to ≈ 5.4, the spectra are symmetrical doublets (Fig. 2e) and can be reproduced using only one quadrupole component. Fig. 3 gives the variation versus x ($8.4 > x > 5.4$) of the isomer shifts and quadrupole splittings refined for the different sites.

Let us consider first the $8.4 \geqslant x \geqslant 5.9$ region. For the two sites, the isomer shift (δ) increases upon oxidation, i.e. with decreasing lithium content (Fig. 3). This variation reflects the progressive replacement of Sn–Li contacts (Li-rich alloys) by Sn–Sn ones (Li-poor alloys), in agreement with the Li–Sn system study of Dunlap [19]. Concerning now the quadrupole splitting (Δ) evolution, it can be seen (Fig. 3) that the site with the smallest isomer shift (site 1) has first the smallest quadrupole splitting and that, upon oxidation, the situation reverses in the vicinity of $x = 7.2$. This crossover is related to the change of the doublet asymmetry: the line located at the highest velocity is first less intense (Fig. 2c) and, below $x \approx 7.2$ (Fig. 2d), becomes more intense than the line located at the lowest velocity. We already observed in the same composition region ($7.0 < x < 7.5$) a similar change of the spectra asymmetry during the reduction of the SnO_2 electrode [1], which denotes in this composition region some reversibility of the phenomenon. This asymmetry change also appears between the spectra reported by Dunlap for Li_5Sn_2 and Li_7Sn_3 [19]. It could thus be expected that some similarity exists between the species formed in our system and the alloys described by Dunlap [19], but, as we already observed during the reduction of the SnO_2 electrode [1], they are not perfectly identical since the isomer shifts and quadrupole splittings values we refined in this region (Fig. 3) are somewhat different than those reported by Dunlap [19] for the corresponding well-defined Li_5Sn_2 and Li_7Sn_3 alloy phases (such differences are not surprising since our alloys are poorly organized, as shown by the X-ray diffractograms, and probably non-stoichiometric).

As indicated above, the smaller the lithium content of Li_ySn alloys, the greater their isomer shift. Consequently, site 2 corresponds to species with smaller lithium content than site 1 ($\delta 2 > \delta 1$). Fig. 4 displays the variation upon oxidation of the relative contributions of sites 1 and 2 to the total absorption area. The curves exhibit a discontinuity between $x = 7.6$ and 7.1, i.e. in the region concerned by the quadrupole splitting crossover. This crossover reveals some structural rearrangement, which means that sites 1 and 2 do not correspond to the same species before and after this transition. However, the general trend (Fig. 4) is clearly that, upon lithium extraction, the contribution of the Li-richer component (site 1) decreases to the benefit of the Li-poorer component (site 2), which is quite logical. At the same time, both $\delta 1$ and $\delta 2$ increase (Fig. 3). It means that oxidation does not result in the simple transformation of species 1 ($Li_{y1}Sn$) into species 2 ($Li_{y2}Sn$, $y2 < y1$) because, in this case, $\delta 1$ and $\delta 2$ would remain constant and only the relative contributions vary. It can thus be deduced that, concomitant with transformation of species 1 into species 2, both types of species become Li poorer and poorer.

From $x \approx 5.7$ ($Li_{1.7}Sn$) to $x \approx 5.4$ ($Li_{1.4}Sn$, the minimum of the NormAbs curve, cf. Fig. 1), site 1 can no longer be detected and the spectra can be reproduced with a unique component corresponding to site 2 (Fig. 2e). In this

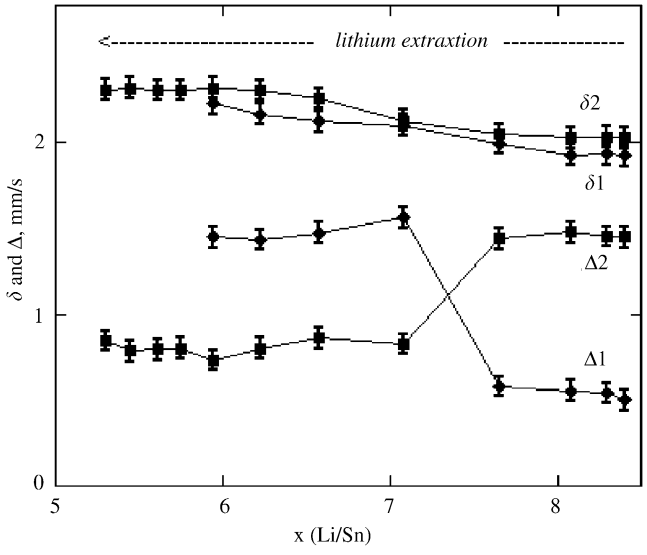

Fig. 3. Variation of the isomer shifts and quadrupole splittings of the two Li_ySn alloy components during lithium extraction from the initial $Li_{4.4}Sn$. The lines are guide for the eyes.

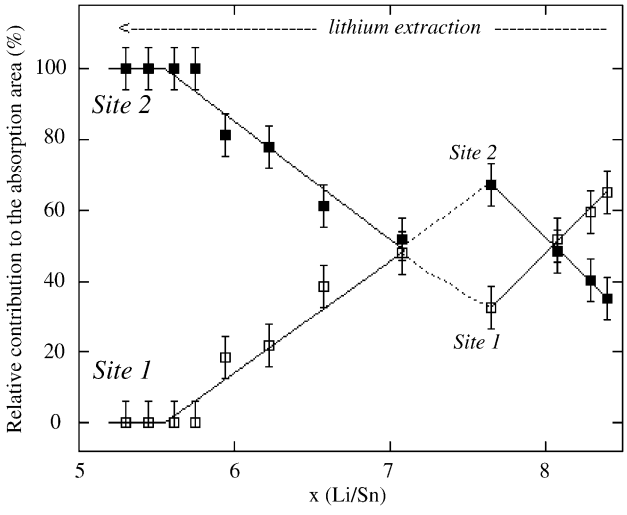

Fig. 4. Variation of the relative contributions of the two Li_ySn alloy components to the total absorption area during lithium extraction from the initial $Li_{4.4}Sn$.

composition region, two mechanisms can be envisioned for the electrode oxidation: the Li_ySn species corresponding to site 2 could (i) progressively release lithium (progressive y decrease from 1.7 to 1.4), which should result in the progressive increase of $\delta 2$ (but in this region, the slope of the $\delta = f(x)$ curve is so weak that it is impossible to decide whether this increase occurs or not), or (ii) transform into new Li-very poor or Li-free (Sn(0)) entities according to a two-phase-like mechanism, and in this case the spectra should contain decreasing contribution of the remaining $Li_{1.7}Sn$ along with increasing contribution of a new site related to the formed entities (but we do not observe any new component, which does not prove the absence of new Li-very poor or Li-free species since their f factor can be expected to be very weak). The spectra thus do not allow a choice to be made between these two possibilities. Neither does the NormAbs variation, since its decrease from $x = 5.7$ to 5.4 can be explained by the two reactional paths we envisioned. According to the first one, a progressive decrease of the lithium content in the alloy would decrease the f factor, and consequently NormAbs, as already discussed above. According to the second one, the amount of site 2 $Li_{1.7}Sn$ species, which contribute to the Mössbauer absorption, would decrease for the benefit of $Li_\varepsilon Sn$ or Sn(0) entities, which perceptibly would not, due to very small f value, and this mechanism would also result in NormAbs decrease. It follows that the experimental data cannot allow to choose between the two mechanisms we proposed. At the limit of this region ($x = 5.4$, the NormAbs minimum), tin can thus be involved in (i) a unique type of species ($Li_{1.4}Sn$) or (ii) several types of species ($Li_\varepsilon Sn$ and/or Sn(0), absent in the spectra, and untransformed $Li_{1.7}Sn$, present in the spectra). For this reason, the species responsible for the resonant absorption at $x = 5.4$ will be hereafter designated by $Li_{1.7/1.4}Sn$.

3.3. The formation of Sn(0) and oxidized species Sn(II) and Sn(IV), $5.4 > x > 3.6$

For x diminishing from 5.4 to 4.3, the NormAbs increase shows that some Sn-containing entities are transformed into new ones with higher f factor. On this simple basis, new contribution(s) can then be expected to appear. Effectively, starting from the first spectrum ($x = 5.1$) we recorded after the NormAbs minimum, the spectra (e.g. Fig. 2f) can be correctly reproduced considering the coexistence of three quadrupole doublets. The first one corresponds to remaining $Li_{1.7/1.4}Sn$ (site 2, $\delta = 2.32$ mm/s, $\Delta = 0.78$ mm/s). The other two (doublets a and b) have rather close isomer shifts ($\delta a \approx 2.1$–2.2 mm/s, $\delta b \approx 2.2$–2.3 mm/s) and largely different quadrupole splittings ($\Delta a \approx 0.6$ mm/s, $\Delta b \approx 2$ mm/s); their attribution will be discussed hereafter. Due to the unresolved character of the concerned spectra, the position parameters (δ and Δ) of these three components were not meaningfully refined. They were consequently fixed, and only the relative contributions refined. Even if such a procedure cannot give very precise results since it does not take into account possible weak variations of δ and Δ, these refinements evidence a progressive decrease of the $Li_{1.7/1.4}Sn$ contribution, for the benefit of doublets a and b (Fig. 5). It means that the $Li_{1.7/1.4}Sn$ alloy transforms into Li-poorer or Li-free species which give rise to doublets a and b. Some contribution to doublets a and b could also arise from transformation of species eventually present in the electrode at $y = 1.4$ ($x = 5.4$) but unobserved in the spectra due to low f value. Identification of the species responsible for the quadrupole doublets a and b is not straightforward, because the δa and δb values do not correspond to usual species whose presence could be anticipated. On the one hand, these values are much too large for Sn(IV) ($\delta \approx 0.00$ mm/s in SnO_2 [20]), on the other hand, they are too small for the usual forms of Sn(II) ($\delta = 2.64$ mm/s in blueblack stable SnO [21]) and metallic tin ($\delta = 2.56$ mm/s in β-Sn [20]). They are also too small to be related to Li-very poor Li_ySn alloys. Besides, it has to be kept in mind that β-Sn (and low lithium content Li_ySn alloys as well) can give only very weak, possibly unobservable, contributions due to their very low f value (attempts to introduce in the calculations a β-Sn component were not conclusive: the contribution is always found to be weak and, if refined, the isomer shift deviates, sometimes largely, from the 2.56 mm/s expected value). It can thus be concluded, in agreement with the results concerning reduction of the SnO_2 electrode [1], that unusual species have been formed. The question is then, what are these unusual species? (This question could not be precisely answered in our previous paper [1]. Effectively, during the reduction process and in the corresponding x range, a large part of the resonant absorption is due to an important contribution of unreacted SnO_2, whose f factor is rather high. Due to the unresolved character of the spectra, the number of minor

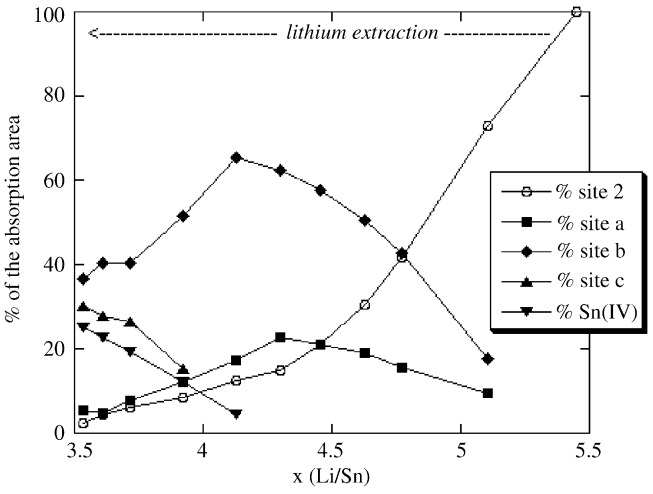

Fig. 5. Variation of the relative contributions of the different subspectra vs. x in the second part of the oxidation process ($x < 5.4$). Site 2 corresponds to $Li_{1.7/1.4}Sn$. Sites a and b are proposed to correspond, respectively, to Sn(0) and oxygen-surrounded Sn(II), both possibly in interaction with Li_2O. Site c corresponds to red SnO-like entities. The error bar is 5%.

contributions, and with greater reason their Mössbauer parameters, remained questionable. It was obvious that only unusual species could be responsible for these minor contributions, but only roughly could their nature be discussed [1].)

Site *b* has an important quadrupole splitting ($\Delta \approx 2$ mm/s) and an isomer shift ($\delta \approx 2.2$–2.3 mm/s) close by the lowest values reported for Sn(II) in the oxygen environment [22]. Such a parameter set can be attributed to oxygen-surrounded Sn(II), whose lone electron pair exhibits, due to crystal field effects, an important p_z character. This configuration is far away from the spherical symmetry of a pure s^2 state; it thus induces an important electric field gradient at the tin nucleus and, consequently, a large Δ value. This important *p* character results in a reduced *s* electron density at the nucleus and, consequently, can explain a reduced isomer shift which in this case can then be as low as 2.2 mm/s (2.26 mm/s at 77 K), as discussed by Flinn [22]. Site *b* can thus be proposed to correspond to Sn(II) sitting in a very asymmetric oxygen environment, probably in ultra-fine and poorly organized particles possibly in interaction with surrounding Li_2O entities. Site *b* contribution reaches $\approx 65\%$ of the total absorption area for $x = 4.13$. However, the effective proportion of the corresponding entities is surely largely smaller since 4.13 is largely greater than 2, the *x* value theoretically corresponding to total transformation into Sn(II). It means that, in the spectra, this component is amplified by a relatively high *f* factor, which can possibly be due to strong interactions with Li_2O (in relation with the small particle size). Less-oxidized entities are thus necessarily present in a noticeable amount, even if they do not appear as a major contribution due to low *f* value.

Site *a* is characterized by a much smaller quadrupole splitting value (≈ 0.6 mm/s). According to Flinn [22], and keeping in mind its low δ value ($\delta \approx 2.1$–2.2 mm/s), such a site can thus hardly be attributed to Sn(II). Its isomer shift, intermediate between those of β-Sn (2.56 mm/s [20]) and α-Sn (≈ 2 mm/s [20]), could correspond to Sn(0)-containing species whose *f* factor could be enhanced, with respect to α- or β-Sn, by strong interactions with Li_2O.

For $x < 4.3$ (Fig. 2g), a shoulder appears in the vicinity of $v = 0$ mm/s, which indicates that Sn(IV) begins to be formed. The corresponding subspectrum is not resolved and, for this reason, its position parameters (δ and Δ) cannot be refined. Its contribution to the absorption area is first very weak ($\approx 5\%$ for $x = 4.13$), which means that the Sn(IV) proportion is still weaker because, if compared to Sn(II) and Sn(0), Sn(IV) can be expected to have a much larger *f* factor. Upon further lithium extraction, this component becomes more important but remains unresolved even at the end of the oxidation process ($x = 3.6$, Fig. 2h). At this stage, its contribution amounts to more than 20% of the total absorption area, but, as discussed above, the effective Sn(IV) proportion is surely smaller due to the *f* values, and consistent with stoichiometry considerations. Effectively, if total oxidation (extraction of 4.8 Li) resulted in the formation of only Sn(0) and Sn(IV), according to the equation

$$Li_{4.4}Sn + 2\ Li_2O \rightarrow 0.9\ Sn(0) + 0.1\ SnO_2 + 1.8\ Li_2O + 4.8\ Li,$$

Sn(IV) would represent only 10% of the total tin amount. Considering that Sn(II) also forms (doublet *a*, and doublet *c* discussed below), the effective Sn(IV) proportion can only be smaller. It is thus clear that oxidation into Sn(IV) is only a minor phenomenon, largely amplified in the spectra due to the high *f* factor.

For the spectra with Sn(IV) component ($x < 4.3$), refinement attempts evidence important correlations between the parameters of the different subspectra. For instance, for $x = 3.6$ (i.e. at the end of the oxidation), excellent reproductions of the experimental spectrum can be obtained with $\delta_{Sn(IV)}$ and $\Delta_{Sn(IV)}$ values, respectively, ranging from 0.10 to 0.22 mm/s and from 0.38 to 0.60 mm/s, and similar dispersion of the parameters related to the other subspectra, depending upon the values chosen as the starting parameters of the refinements. For this reason, it is impossible to decide which of the refined parameter set is really the correct one. However, even if the precise parameter values cannot be determined, several conclusions can be drawn concerning this region ($4.3 > x > 3.6$).

(i) The contribution of residual $Li_{1.7/1.4}Sn$ alloy decreases (Fig. 5). For $x < 3.7$, the spectra can be correctly reproduced without this component, whose existence thus becomes questionable.

(ii) The absorption at v slightly greater than 0 (0.10–0.22 mm/s) can only be due to Sn(IV), but it does not correspond exactly to reformation of the pristine SnO_2 ($\delta = -0.02$ mm/s [1]) we used for manufacturing our electrode, the increased isomer shift being possibly due to non-stoichiometry and/or structural defects eventually related to interactions with Li_2O. This contribution logically increases upon oxidation (Fig. 5).

(iii) Three other contributions are also present in these spectra. Two of them are similar to doublets *a* ($\delta \approx 2.1$–2.3 mm/s, $\Delta \approx 0.4$–0.6 mm/s) and *b* ($\delta \approx 2.2$–2.3 mm/s, $\Delta \approx 2.0$–2.2 mm/s) discussed above and are, respectively, attributed (with some prudence) to Sn(0)-containing entities and Sn(II)–O fragments, both possibly in interaction with Li_2O. The third of these contributions (doublet *c*) exhibits a larger isomer shift ($\delta \approx 2.5$–2.6 mm/s) and important quadrupole splitting ($\Delta \approx 1.8$–2.2 mm/s). The δ value, larger than that of doublet *b*, suggests the presence of more usual Sn(II)–O species, possibly Sn(II)–O species with reduced (or without) interactions with Li_2O. More precisely, this isomer shift is not very different from that in stable crystalline SnO (blueblack variety, $\delta = 2.64$ mm/s [21]), which indicates that the *s* electron densities at the nucleus and, consequently the *p* populations, are rather comparable. Nevertheless, despite this isomer shift similarity, species responsible for doublet *c* do not correspond to the atomic arrangement of stable crystalline SnO

because the quadrupole splittings are significantly different ($\Delta \approx 1.8$–2.2 mm/s for doublet c and $\Delta = 1.3$ mm/s for SnO [21]). This structural difference is probably associated with spin–orbit-coupling effects. Indeed, according to the $\delta = f(\Delta)$ diagram drawn by Flinn [22], the relatively small Δ value observed in blueblack SnO is due to the important spin–orbit coupling, which, for a given total p population, reduces the p_z density and, consequently, the quadrupole splitting. Considering the same $\delta = f(\Delta)$ diagram, the δ and Δ parameters of doublet c can be thought to correspond to species in which, compared to stable SnO, the proportion of the p population involved in the p_z state (and, in consequence, Δ) is more important due to weaker spin–orbit coupling. In fact, parameters of doublet c fairly correspond to those in the red metastable variety of SnO ($\delta = 2.52$ mm/s and $\Delta = 2.02$ mm/s [23]). It can thus be proposed that doublet c is due to entities in which tin sits, as in red SnO [24], in pseudo-tetrahedral coordination constituted by its lone electron pair (E) and three oxygen atoms, according to a $3+E$ geometry (instead of $4+E$ geometry in blueblack stable SnO [25]). $3+E$ geometry was also evidenced for ^{119}Sn(II) located at the surface of Cr_2O_3, and was also found to be associated with a high Δ value (2.10 mm/s [26]), which further supports the structural model we propose. Doublet c cannot be detected at $x = 4.1$ and represents about 30% of the total absorption area at the end of the oxidation ($x = 3.6$) (Fig. 5). The increase of this contribution upon oxidation is consistent with the reduced interactions with Li_2O we envisioned above. Effectively, at low Sn(II) content, the particles are very small and all the Sn(II) species are concerned by interactions with surrounding Li_2O (doublet a); increase of the Sn(II) proportion likely results in some increase of the corresponding particle size, and significant contribution of core unperturbated red SnO-like entities can then be observed (doublet c).

Besides, it is to be stressed again that, even if we did not evidence β-Sn contribution, its existence could escape notice due to its low f value (this is also true for other eventual species with low f factor).

3.4. Recapitulation of the different steps: what is observed vs. what could be expected to occur

Simple observation of the variation of the resonant absorption area (NormAbs) vs. the lithium content (Fig. 1) shows that the oxidation of our electrode proceeds in two reaction steps. The second one begins at $x = 5.4$, i.e. largely before the total removal of lithium from the alloys is achieved ($x = 4$, Fig. 6a).

Starting from this first approach, discussion of the parameters refined for the different spectra allows the oxidation process to be precised and summarized as follows (Fig. 6b).

The beginning of the oxidation consists of simple extraction of lithium from the Li_ySn alloys, with progressive y decrease from 4.4 ($x = 8.4$) to 1.7 ($x = 5.7$). The mechanism is possibly more complex from $Li_{1.7}Sn$ ($x = 5.7$) to $Li_{1.4}Sn$ ($x = 5.4$). For this reason, the alloy responsible for the resonant absorption at $y = 1.4$ ($x = 5.4$, the end of the first part of the NormAbs curve) is represented by the formula $Li_{1.7/1.4}Sn$.

Starting from $x = 5.4$ and down to $x \approx 4.3$–4.1 (Fig. 5), the $Li_{1.7/1.4}Sn$ alloy (site 2) progressively transforms into Sn(0) (site a) and Sn(II) in a low symmetry oxygen environment (site b), both probably in interaction with the surrounding Li_2O.

The contributions of these Sn(II) and Sn(0) entities then diminish ($x < 4.3$–4.1, Fig. 5), and a new type of Sn(II) appears with a local structure related to that in the red metastable variety of SnO. Nearly at the same time a Sn(IV) contribution appears, which does not correspond exactly to that of the tin dioxide used for the battery manufacturing, likely due to non-stoichiometry and/or structural defects eventually related to interactions with Li_2O. Some unreacted $Li_{1.7/1.4}Sn$ remains present nearly till the end of the oxidation.

The three-step mechanism described above is based on intensity variations of the different contributions involved. However, it would be hazardous to propose a quantitative mechanism since the f factors are not known and since some low f contributions can escape notice, which precludes the relative amounts of the various reaction products to be derived from the corresponding relative contributions to the total absorption area.

Fig. 6 shows that the oxidation mechanism deduced from our results (Fig. 6b) significantly differs from the simplest scheme which could have been envisioned (Fig. 6a). In this respect, an interesting question to be answered is why do Sn(II) and Sn(IV) begin to appear before the Li_ySn alloys have been completely transformed into Sn(0), contrary to the logical scheme envisioned (Fig. 6a) assuming the cell to be at every moment close by thermodynamic equilibrium, at least down to $x = 4$. Due to the dynamic character of our study, and also due to the poor crystalline organization of the reaction products, the Li_ySn alloys evidenced by our Mössbauer results cannot be claimed to be exactly identical to the well-defined phases studied by Dunlap et al. [19]. However, it can be anticipated that, for similar composition, the local atomic arrangement in our alloy species should be rather similar to that in the crystalline samples. On this basis, it can be thought that the answer to the question asked above probably lies in both structural and nanostructural features, as will be discussed below.

The physico-chemical characteristics of crystalline Li_ySn alloys allow two families to be distinguished: the family of Li-rich ($Li_{22}Sn_5$, Li_7Sn_2, $Li_{13}Sn_5$, Li_5Sn_2, and Li_7Sn_3) and that of Li-poor (LiSn, Li_2Sn_5, and, by extrapolation, β-Sn) alloys. Lithium-rich alloys have close melting points (around 700 °C) and close crystallographic structures based on a bcc subcell ($a \approx 3.3$ Å). Moreover, for this family, the average number of Sn–Sn bonds per Sn atom is very weak (≈ 0 for $Li_{22}Sn_5$, increasing to 1.3 for Li_7Sn_3), which results

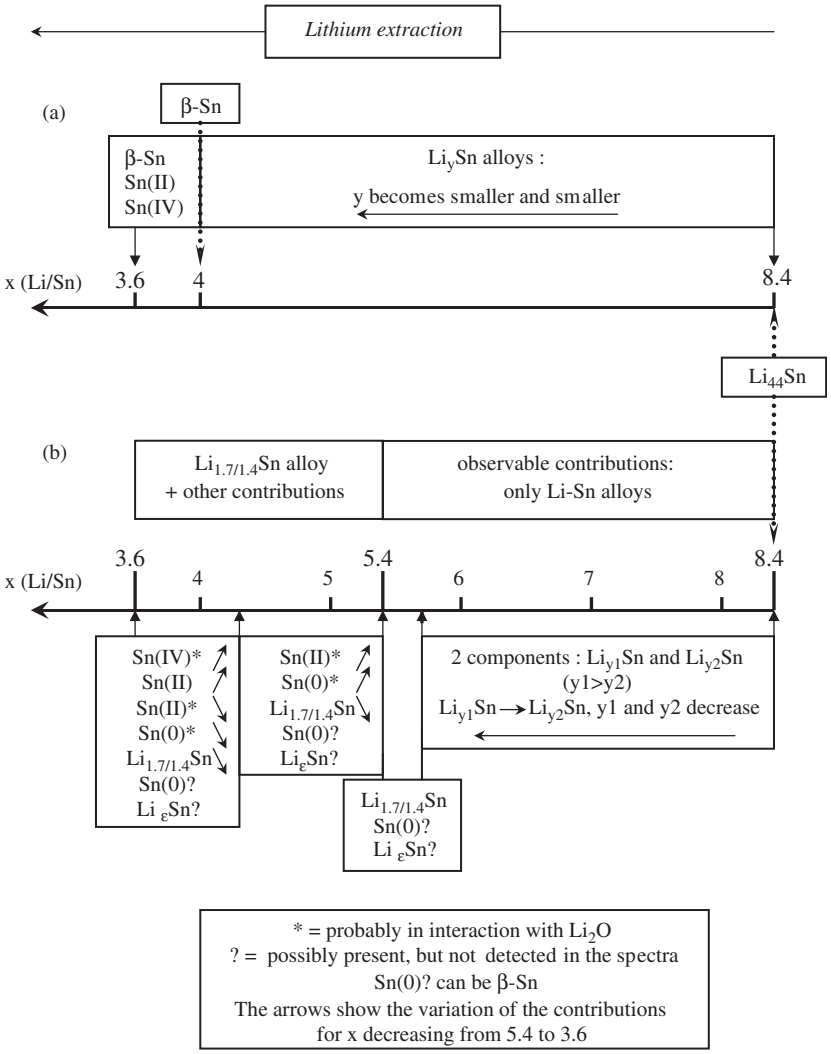

Fig. 6. The successive steps of oxidation of the previously reduced SnO_2 electrode: what could be expected on the basis of Refs. [2–4] (a), and what can be deduced from our measurements (b).

in a shielding of every tin atom by its lithium neighbors [19,27,28]. Lithium-poor alloys have lower melting points (e.g. 486 °C for LiSn) and their structure is completely different: they can be seen as layered compounds with, in every layer, an ordered arrangement of the two elements. Of course, for stoichiometry reasons, the order geometry depends upon the composition, but the structural framework remains exactly the same (including β-Sn). In particular, for this family, the average number of Sn–Sn bonds per Sn atoms is important (4 for LiSn instead of 1.3 for Li_7Sn_3). It follows that transition from the former to the latter family requires drastic structural rearrangement.

Another parameter to be considered in this respect is V, the alloy volume per Sn atom, and its variation versus the alloy composition. At decreasing lithium content, the volumic change associated with the transition from each alloy (i) to the following one $(i+1)$ can be represented by $\boldsymbol{r}$, the contraction factor $(V(i+1) = V(i)/\boldsymbol{r})$, which is given below, in brackets, between the formulae of the concerned consecutive alloys:

Li-rich family : $Li_{22}Sn_5$ (1.20) Li_7Sn_2 (1.23) $Li_{13}Sn_5$ (1.02) Li_5Sn_2 (1.05) Li_7Sn_3,

Transition from Li-rich to Li-poor family:

Li_7Sn_3 (1.49) LiSn,

Li-poor family : LiSn (1.24) Li_2Sn_5 (1.22) $\beta - Sn$.

The contraction factor is obviously greater for the transition from Li_7Sn_3 to LiSn than for any other transition, which fairly illustrates the abruptness of the rearrangement that can be expected to occur in this composition region.

Now, the alloy formula for which Sn(II) and Sn(IV) begin to appear in our electrode ($Li_{1.7/1.4}Sn$) is just intermediate between Li_7Sn_3 ($Li_{2.33}Sn$) and LiSn, i.e. just between the Li-rich and Li-poor alloy families. From $y =$ 4.4 to1.7/1.4, i.e. during the first step of the electrode oxidation (Fig. 1), the alloys remain in the Li-rich domain

and, for this reason, lithium extraction results in only slight structural changes. In this region, the electrode oxidation proceeds roughly as expected on the basis of thermodynamic equilibrium, as evidenced by our Mössbauer spectra. Then, upon lithium extraction from $Li_{1.7/1.4}Sn$, the average number of Sn–Sn bonds per Sn atom has to suddenly increase from 1.3 (Li_7Sn_3-like species) to 4 (LiSn-like species) and V to be concomitantly divided by 1.5. This considerable structural rearrangement has to take place at a nanoscopic scale [8] because, due to electrochemical grinding, the tin-containing particles are ultra-fine. In relation with the particle size, the proportion of tin surface atoms, which have in their environment oxygen atoms belonging to neighboring Li_2O particles, is far from being negligible. Formation of Sn(II)–O and Sn(IV)–O species through the reaction of the surface tin atoms with their oxygen neighbors can thus become the dominant phenomenon, since lithium extraction from $Li_{1.7/1.4}Sn$ can be largely hindered due to the importance of the structural change it requires.

These considerations fairly explain why, even if the cell could be expected to work close by thermodynamic equilibrium (very low cycling rate), Sn(II)- and Sn(IV)-containing species appear before the alloys have been completely converted to Sn(0).

4. Conclusion

The present study demonstrates that, as already reported for the reduction of the SnO_2 electrode, the mechanism of its reoxidation is much more complex than anticipated on the basis of thermodynamic equilibrium, even at a very slow cycling rate. Besides, the presence of unusual species was unambiguously established. In particular, the Sn(IV)- and Sn(II)-containing entities do not correspond to the crystalline SnO_2 and SnO (stable blueblack variety) references. All these results confirm that, even at a low charging or discharging rate, a working electrode is far from thermodynamical equilibrium. One can even wonder whether it is really pertinent to speak about thermodynamical equilibrium when such systems consisting of ultra-fine particles are concerned.

Acknowledgments

The authors thank Dr. Mathieu Morcrette from Laboratoire de Réactivité et de Chimie des Solides, Unité de Prototypage UMR 6007 CNRS, Amiens, for the cell preparation. Dr. Philippe Deniard and Dr. Dominique Guyomard (Laboratoire de Chimie des Solides, Institut des Matériaux Jean Rouxel) are also acknowledged for their help with the electrochemical tests.

References

[1] I. Sandu, T. Brousse, D.M. Schleich, M. Danot, J. Solid State Chem. 177 (2004) 4332.
[2] I.A. Courtney, J.R. Dahn, J. Electrochem. Soc. 144 (1997) 2045.
[3] I. Sandu, T. Brousse, J. Santos-Peña, M. Danot, D.M. Schleich, Ionics 8 (2002) 27.
[4] I.A. Courtney, R.A. Dunlap, J.R. Dahn, Electrochim. Acta 45 (1999) 51.
[5] D. Guyomard, J.-M. Tarascon, US Patent 5,192,629 (1993).
[6] C.J. Wen, R.A. Huggins, J. Solid State Chem. 35 (1980) 376.
[7] G.R. Goward, N.J. Taylor, D.C.S. Souza, L.F. Nazar, J. Alloys Compd. 329 (2001) 82.
[8] P. Poizot, S. Laruelle, S. Grugeon, L. Dupont, J.-M. Tarascon, Nature 407 (2000) 496.
[9] G. Grube, E. Meyer, Z. Elektrochem. 40 (1934) 771.
[10] D.M. Bailey, W.H. Skelton, J.F. Smith, J. Less-Common Met. 64 (1979) 233.
[11] Y. Idota, T. Kubota, A. Matsufuji, Y. Maekawa, T. Miyasaka, Science 276 (1997) 1395.
[12] I.A. Courtney, J.R. Dahn, J. Electrochem. Soc. 144 (1997) 2045.
[13] I.A. Courtney, J.R. Dahn, J. Electrochem. Soc. 144 (1997) 2947.
[14] R. Retoux, T. Brousse, D.M. Schleich, J. Electrochem. Soc. 146 (1999) 2472.
[15] T. Brousse, R. Retoux, U. Herterich, D.M. Schleich, J. Electrochem. Soc. 145 (1998) 1.
[16] W. Liu, X. Huang, Z. Wang, H. Li, L. Chen, J. Electrochem. Soc. 145 (1998) 59.
[17] J. Morales, L. Sanchez, J. Electrochem. Soc. 146 (1999) 1640.
[18] F. Belliard, P.A. Connor, J.T.S. Irvine, Solid State Ionics 135 (2000) 163.
[19] R.A. Dunlap, D.A. Small, D.D. MacNeil, M.N. Obrovac, J.R. Dahn, J. Alloys Compd. 289 (1999) 135.
[20] N.N. Greenwood, T.C. Gibb, Mössbauer Spectroscopy, Chapman & Hall, London, 1971, p. 374.
[21] R.H. Herber, Phys. Rev. B 27 (7) (1983) 4013.
[22] P.A. Flinn, in: G.K. Shenoy, F.E. Wagner, (Eds.), Mössbauer Isomer Shifts, North-Holland Publishing Company, Amsterdam, New York, Oxford, 1978, 606pp.
[23] S. Maingaud, P.B. Fabritchnyi, M. Danot, unpublished results.
[24] A.J.F. Boyle, D.St.P. Bunbury, C. Edwards, Proc. Phys. Soc. 79 (1962) 416.
[25] W.J. Moore, L. Pauling, J. Am. Chem. Soc. 63 (1941) 1392.
[26] M.I. Afanasov, M. Danot, A.A. Ryabchikov, S. Maingaud, P.B. Fabritchnyi, J. Rouxel, Mater. Res. Bull. 31 (5) (1996) 465.
[27] U. Frank, W. Müller, Z. Naturforsch. 30b (1975) 316.
[28] I.A. Courtney, J.S. Tse, Ou Mao, J. Hafner, J.R. Dahn, Phys. Rev. B 58 (1998) 15584.